Eur. J. Mech., B/Fluids, **17**, n° 1, 1-18, 1998

Benjamin-Feir and Eckhaus instabilities with galilean invariance: the case of interfacial waves in viscous shear flows

P. BARTHELET and F. CHARRU

ABSTRACT. – We consider the stability of interfacial waves in a two-layer viscous shear flow. The weakly nonlinear dynamics are governed by a set of two coupled amplitude equations (Renardy and Renardy, 1993): a complex Ginzburg-Landau equation for the travelling wave with finite wavenumber k_c, and a Burgers-type equation for the neutral mode with wavenumber $k = 0$. We study here the linear stability, against long wavelength disturbances, of the travelling wave solutions of these equations. For the travelling wave with $k = k_c$, the Lange & Newell criterion for the Benjamin-Feir instability is modified by the coupling, and a new kind of instability may arise from the neutral mode $k = 0$. For travelling waves with $k \neq k_c$, several wavenumber bands may be Eckhaus-unstable, with growth rate much larger than for the classical Eckhaus instability. A physical mechanism for this instability is proposed. Beyond the case of interfacial waves in viscous shear flows, the results apply for physical systems with translational and galilean invariances, and no-space-reflection symmetry. © Elsevier, Paris.

1. Introduction

Numerous dissipative systems are known to bifurcate from a uniform stationary state to a periodic spatial structure, when the bifurcation parameter is increased beyond some critical value. In hydrodynamics, the Rayleigh-Bénard convection and the Taylor-Couette flow are among the most studied. Interfaces in shear flows may also exhibit interesting low Reynolds number instabilities, leading to finite amplitude travelling waves. As the bifurcation parameter is increased, the periodic structures born from the primary bifurcation, such as convective rolls or travelling waves, become unstable in turn, leading to another stationary or to a time-dependent pattern (Newell, Passot and Lega, 1993).

In extended geometries, weak gradients of the amplitude of the periodic structure may generate large scale mean fields, which may in turn enhance or inhibit secondary instabilities of the periodic structure. In the Rayleigh-Bénard convection, this slowly-varying mean field is an horizontal drift flow with vertical vorticity (Pocheau and Daviaud, 1997; Zippelius and Siggia, 1983). Similarly, the convection in binary fluid mixtures involves the coupling of the wave amplitude with the mean concentration field (Riecke, 1992).

Institut de Mécanique des Fluides de Toulouse, UMR CNRS/INPT-UPS 5502, 2, allée du Professeur Camille Soula, 31400 Toulouse, France.

EUROPEAN JOURNAL OF MECHANICS, B/FLUIDS, VOL. 17, N° 1, 1998
0997-7546/98/01/© Elsevier, Paris

The stability of travelling interfacial waves in two-layer Couette-Poiseuille flows (*Fig.* 1) crucially involves the coupling with a neutral long wave mode. The corresponding set of two coupled amplitude equations has been derived by Renardy and Renardy (1993): it consists of a complex Ginzburg-Landau (CGL) equation for the amplitude of the weakly unstable finite-wavenumber mode, and a Burgers equation for the amplitude of the neutral zero-wavenumber mode. In this paper, we study the linear stability of the travelling wave solutions of these coupled equations. It turns out that the classical Benjamin-Feir and Eckhaus instabilities are qualitatively modified by the coupling. As the Renardys' equations are normal forms for systems with translational and galilean invariance (Coullet and Fauve, 1985), our results may apply to other physical situations.

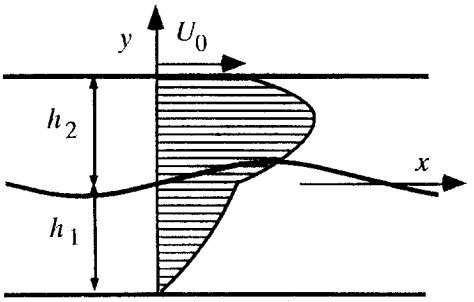

Fig. 1. – Sketch of the Couette-Poiseuille flow.

At the end of this section, we briefly review linear stability results, and some experimental results. In section 2, the two amplitude equations for interfacial instabilities of the two-layer Couette-Poiseuille flow are presented. In section 3, travelling wave solutions are given, and the eigenvalues governing their linear stability are obtained. Instability criteria are discussed in section 4. The results are summarised and discussed in section 5, and extented to more general systems with same symmetries.

1.1. Linear stability results and symmetries

The interface between two viscous fluid layers in two-dimensional Couette-Poiseuille flow (*Fig.* 1) may be unstable against long wavelength disturbances ($k \equiv 2\pi h_1/\lambda \ll 1$) or against finite wavelength disturbances ($k = O(1)$). Stability or instability depend on the six dimensionless flow parameters: the viscosity ratio and the density ratio of the fluids, the Reynolds number of each fluid layer, and the Weber and Froude numbers which take into account the stabilizing effect of surface tension and gravity, respectively.

For long waves, the dispersion relation for normal modes $\exp(st - ikx)$, with real k and $s = \sigma + i\omega$, can be found from a regular perturbation expansion in the small wavenumber (Yih, 1967):

$$\sigma(k) = -\tilde{\chi} k^2 - S k^4 + O(k^6) \tag{1a}$$

$$\omega(k) = c_0 k + O(k^3) \tag{1b}$$

where $\tilde{\chi}$, S and c_0 depend on the flow parameters. The wave velocity c_0 is non-zero, and this corresponds to the non invariance of the basic flow under the space-reflection symmetry $x \to -x$. The growth rate $\sigma(k)$ shows that long waves are stable if $\tilde{\chi} > 0$ or unstable if $\tilde{\chi} < 0$, and that short waves are stabilized by surface tension, see Figure 2*a* (S involves the Weber number and is always positive). Typically, long waves are unstable when the thinner layer is the more viscous (Hooper, 1985).

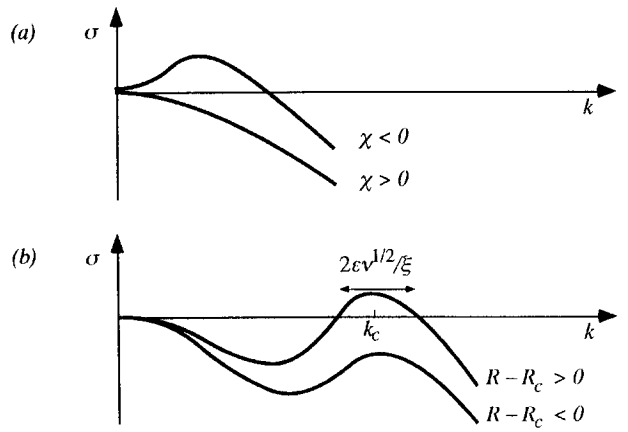

Fig. 2. – (*a*): Growth rate $\sigma(k)$ for stable and unstable long waves. (*b*): Growth rate $\sigma(k)$ when long waves are stable. The mode $k = 0$ is always neutral. For $R = R_c$, the mode $k = k_c$ is marginally stable.

Furthermore, (1a) shows that the normal mode with wavenumber $k = 0$ is always neutral. This mode corresponds to a vertical shift of the whole interface, and it is neutral owing to mass conservation. Indeed, for incompressible flows, the kinematic (or no-mass transfer) condition at the interface can be written as:

$$\frac{\partial \eta}{\partial t} + \frac{\partial \Psi_1(\eta)}{\partial x} = 0 \tag{2a}$$

where $\eta(x, t)$ is the interface displacement and $\Psi_1(\eta)$ is the stream fonction of the lower fluid at the interface. As $\Psi_1(\eta)$ represents the flow rate of the lower fluid, (2a) also represents the mass conservation equation integrated over the thickness of the lower fluid. The Fournier transform of (2a) immediately shows that the mode with $k = 0$ must be neutral.

From the point of view of symmetries, the existence of the neutral mode $k = 0$ is related to the galilean invariance of the system (Coullet and Fauve, 1985). Indeed, for long waves ($k \ll 1$) and for moderate surface tension effects (Weber number $We = O(k)$), the normalized streamfunction is (Charru and Fabre, 1994; Hooper and Grimshaw, 1985):

$$\Psi_1(\eta) = a_1 \eta + \eta^2 + a_2 \eta_{,x} + \text{h.o.t.} \tag{2b}$$

Thus, dominant terms in the mass conservation Eq. (2a) gives the Burgers equation, which is invariant under the "galilean" transformation:

$$x \to x - ut, \qquad \eta \to \eta - u.$$

Strictly speaking, the above transformation is not the true galilean transformation since η is not the longitudinal velocity but the vertical displacement of the interface. However it can be considered as a generalized galilean transformation.

Besides the long waves instability and the $k = 0$ neutral mode, numerical resolution of the linearized eigenvalue problem shows that there may exist a finite wavenumber instability (Renardy, 1985). This instability occurs for a critical value R_c of the bifurcation parameter R, for which the normal mode with finite wavenumber k_c is marginally stable. The bifurcation parameter R may be the Reynolds number of one of the fluid layers, or the viscosity ratio, or any other flow parameter. Above R_c, the basic flow is unstable against a band of wavenumbers centered at k_c (*Fig. 2b*). The eigenvalues $s = \sigma + i\,\omega$ associated with this continuum of unstable modes are given by the Taylor expansion of the dispersion relation around the eigenvalue crossing the imaginary axis for $R = R_c$:

$$\sigma(k) = \nu\varepsilon^2 - \xi^2 (k - k_c)^2 + \text{h.o.t.} \tag{3a}$$

$$\omega(k) - \omega_c = c_g (k - k_c) - \xi^2 c_1 (k - k_c)^2 + \text{h.o.t.} \tag{3b}$$

$$\text{with} \quad \varepsilon^2 \equiv (R - R_c)/R_c \ll 1.$$

All coefficients are $O(1)$. ω_c is the angular frequency of the critical mode, $c_g = c_g(k_c)$ is the group velocity, ξ is the correlation length and c_1 describes dispersive effects. These coefficients can be obtained numerically or from a small Reynolds number perturbation expansion (Albert, 1996). The bandwidth of the unstable wavenumbers is $2\,\varepsilon\nu^{1/2}/\xi$, and in the $(k - k_c,\ R - R_c)$ plane, the marginal stability curve is the parabola $R - R_c = (R_c\,\xi^2/\nu)(k - k_c)^2$.

Notice that the bifurcation occuring at $R = R_c$ is a Hopf bifurcation: the equations of the problem being real, $s(-k) = s^*(k)$, where the * exponent denotes complex conjugation. Then the eigenvalues of the modes k_c and $-k_c$ cross the imaginary axis of the complex plane simultaneously for $R = R_c$, with angular frequency ω_c and $-\omega_c$, respectively.

1.2. Experimental results

Experiments on a two-layer Couette flow have confirmed the above linear stability results (Barthelet, Charru and Fabre, 1995). These experiments were carried out in a channel of rectangular cross-section bent into an annular ring. The lower fluid was a mixture of water and glycerine, and the upper fluid was mineral oil. For small upper plate velocity, the flat horizontal interface is stable. Above some critical velocity U_c about 0.2 m/s, two types of waves may appear, both supercritically, depending on the thickness ratio $d = h_2/h_1$. For small thickness ratio, a long wave appears with wavelength λ equal to the perimeter of the channel ($\lambda \approx 1.2$ m, $k \equiv 2\,\pi\,h_1/\lambda \approx 0.05$), corresponding to the long wave instability. For thickness ratio close to unity, long waves do not appear, and a much shorter ware arises, with wavenumber $k \approx 1$ and frequency $f \approx 7$ Hz, corresponding to the finite wave instability.

In the latter case, *i.e.* when the basic flow is stable against long waves, and near the threshold of instability, the short wave is nearly sinusoidal and perfectly periodic. Increasing the upper plate velocity above $1.1\,U_c$, the short wave becomes unstable against long wave disturbances. Keeping the upper plate velocity fixed, this instability develops as shown on Figure 3, which displays three parts of a continuous time record of the interface position, at a fixed place in the middle of the channel. Since the channel is closed, the probe "sees" the same wave crest every 4 seconds approximately. Figure 3 shows that the short wave seems uniform for a few minutes (*Fig.* 3*a*). Then, a long wave variation of the local mean height B of the interface appears, coupled to a pinching of the amplitude A of the short wave (*Fig.* 3*b*). This pinching is locked to the steep front of the long wave B: the group velocity c_g of A and the wave velocity c_0 of B are equal or a least very close. The pinching is also associated with a local shortening of the wavelength. Compression and pinching increase and lead to annihilation of one wavelength and to global dilation of the pattern. Then the periodic structure tends to relax to uniformity, but the above scenario repeats once, leading to the death of one more wavelength. The long wave mode eventually relaxes to zero amplitude, and the short wave recovers uniform amplitude and wavelength (*Fig.* 3*c*) (Barthelet and Charru, 1996).

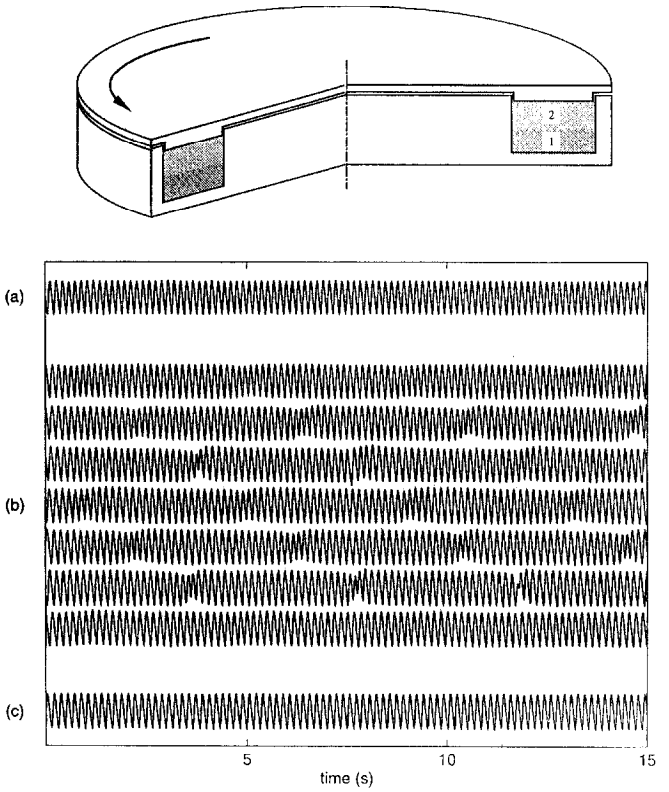

Fig. 3. – Top: Sketch of the experimental device. Bottom: Time evolution of the interface position for $U/U_c = 1.07$; (*a*): uniform short wave at the beginning of the record, after a transient of a few seconds; (*b*): the long wave modulation is clearly visible 120 seconds later, and lead to annihilation of two wavelengths; (*c*): uniform short wave 300 seconds later.

For decreasing velocity, the dynamics are more complicated, with longer transients, and eventually lead to the creation of wavelengths. A detailed account of these secondary instabilities is postponed to another paper.

The secondary instability described above cannot be framed in the classical phase instability mechanism. Clearly, it involves the coupling of the travelling wave with a long wave mode. This corroborates the linear stability results, which show the existence of a neutral zero-wavenumber together with a finite-wavenumber instability (*Fig.* 2).

2. Amplitude equations

The wave packet centered on the weakly unstable mode k_c can be described as a monochromatic wave $A(x, t)\, e^{i(\omega_c t - k_c x)} + \text{c.c.}$, with complex amplitude $A(x, t)$ which may be slowly modulated in space and time. The weakly nonlinear dynamics of this wave packet can be described by a set of two coupled amplitude equations, for the complex amplitude $A(x, t)$ and the real amplitude $B(x, t)$ of the neutral mode $k = 0$. Such a set of amplitude equations has been obtained for the Couette-Poiseuille two-layer flow by Renardy and Renardy (1993), using the center manifold approach of bifurcation theory. These equations involve the scaled variables:

$$\tilde{X} = \varepsilon (x - c_g t), \quad \tilde{T} = \varepsilon^2 t,$$
$$\tilde{A} = \varepsilon^{-1} A, \quad \tilde{B} = \varepsilon^{-2} B.$$

The introduction of the slow variables $\tilde{X}$ and $\tilde{T}$ can be justified as follows. At a distance ε^2 from the threshold of instability, the dispersion relation (3) shows that a packet of linearly unstable waves develops through instability over a timescale of order ε^{-2}. However, dispersion acts on the shorter timescale ε^{-1}. It may induce modulations of the envelope of the wave pattern over a distance of order ε^{-1}, travelling with the group velocity c_g. Thus, the amplitudes A and B are expected to vary over these slow variables. The finite-wavenumber travelling wave arises from a Hopf bifurcation, which is assumed to be supercritical, and its amplitude A is of order ε. Finally, since B is destabilized by A, its amplitude is expected to be of smaller order, and inspection of the equations shows that ε^2 is a good choice. Moreover the latter scaling agrees with experiments, see Figure 3. With these scaling and for two-dimensional disturbances, Renardy's equations are:

$$\text{(4a)} \qquad \frac{\partial \tilde{A}}{\partial \tilde{T}} = \nu \tilde{A} + \xi^2 (1 + ic_1) \frac{\partial^2 \tilde{A}}{\partial \tilde{X}^2} - \gamma_r (1 + ic_2) |\tilde{A}|^2 \tilde{A} + (\kappa_r + i\kappa_i) \tilde{A} \tilde{B}$$

$$\text{(4b)} \qquad \frac{\partial \tilde{B}}{\partial \tilde{T}} = \varepsilon^{-1} \tilde{c} \frac{\partial \tilde{B}}{\partial \tilde{X}} + \tilde{\chi} \frac{\partial^2 \tilde{B}}{\partial \tilde{X}^2} + \varepsilon \tilde{\zeta} \tilde{B} \frac{\partial \tilde{B}}{\partial \tilde{X}} + \varepsilon^{-1} \tilde{\delta} \frac{\partial |\tilde{A}|^2}{\partial \tilde{X}}$$

where $\tilde{c} = c_g - c_0$. All coefficients in Eqs. (4) are real. Since the Hopf bifurcation is assumed to be supercritical, γ_r is positive. When the coupling coefficients are zero, (4a) reduces to the complex Ginzburg-Landau equation (CGL equation), and (4b) reduces

to the Burgers equation (2), which describes weakly nonlinear long waves (Charru and Fabre, 1994; Hooper and Grimshaw, 1985). Note that the linear parts of (4a) and (4b) can be obtained from the inverse Fourier-Laplace transforms of the dispersion relations (1) and (3) (Whitham, 1974): thus, one fourth order spatial derivative term may be added to (4b), taking into account the effect of surface tension. Nevertheless, since long waves are assumed to be linearly stable ($\tilde{\chi} > 0$), this term can be omitted in the present stability analysis.

Normalizing the variables as:

$$\tilde{T} = T/\nu, \quad \tilde{X} = (\xi^2/\nu)^{1/2}\, X,$$
$$\tilde{A} = (\nu/\gamma_r)^{1/2}\, A \exp\left[-i\,\nu\, c_2\, T\right], \quad \tilde{B} = \nu\, B,$$

and discarding the quadratic B-term in (4b) which is of smaller order, (4) become:

$$\frac{\partial A}{\partial T} = (1 + ic_1)\,\frac{\partial^2 A}{\partial X^2} + (1 + ic_2)\,(A - |A|^2 A) + (\kappa_r + i\,\kappa_i)\,AB \tag{5a}$$

$$\frac{\partial B}{\partial T} = \varepsilon^{-1}\, c\,\frac{\partial B}{\partial X} + \chi\frac{\partial^2 B}{\partial X^2} + \varepsilon^{-1}\,\delta\,\frac{\partial |A|^2}{\partial X}. \tag{5b}$$

All terms in (5a) are $O(1)$, but (5b) involves ε^{-1}. As noted by (Renardy and Renardy, 1993), no scaling can remove ε from these equations. We only consider here the case when all terms in (5) have same order, which corresponds to $c = O(\varepsilon)$, $\delta = O(\varepsilon)$. This assumption is justified by the experiments: the velocities of the modulation and of the long wave appear to be the same, so their difference may be assumed of order ε. Then $\delta = O(\varepsilon)$ is needed for consistency of (5b).

3. Travelling waves and stability criterion

Equations (5) admit the family of solutions:

$$A_0(X, T) = (1 - q^2)^{1/2}\, e^{i\left[qX - (c_1 - c_2)\, q^2\, T\right]} \tag{6a}$$

$$B_0(X, T) = 0 \tag{6b}$$

For given q, (6) corresponds to a travelling wave with amplitude $\varepsilon\left[\gamma_r\,(1 - q^2)/\nu\right]^{1/2}$, wavenumber $k = k_c + \varepsilon\,(\xi^2/\nu)^{-1/2}\, q$, and angular frequency $\omega = \omega_c - \varepsilon^2 \nu\, c_1\, q^2$ in the primary reference frame. Only the case $|q| < 1$ needs to be considered, since for $|q| > 1$ the wavenumber k is outside the linearly unstable band.

In order to study the linear stability of (6), we assume the following form for the perturbed amplitudes:

$$A(X, T) = A_0(X, T)\,(1 + a(X, T))$$
$$B(X, T) = b(X, T)$$

Linearizing Eqs. (5), one gets:

$$\frac{\partial a}{\partial T} = i\,(c_1 - c_2)\,q^2\,a + (1 + ic_1)\left[\frac{\partial^2 a}{\partial X^2} + 2\,iq\,\frac{\partial a}{\partial X} - q^2\,a\right] + (1 + ic_2)\,[a - (1 - q^2)\,(2\,a + a^*)] + (\kappa_r + i\,\kappa_i)\,b \tag{7a}$$

$$\frac{\partial b}{\partial T} = (\varepsilon^{-1}\,c)\,\frac{\partial b}{\partial X} + \chi\,\frac{\partial^2 b}{\partial X^2} + (\varepsilon^{-1}\,\delta)\,(1 - q^2)\,\frac{\partial\,(a + a^*)}{\partial X} \tag{7b}$$

where the * exponent denotes complex conjugation. Then, one looks for normal mode solutions with wavenumber p:

$$a = a_1\,e^{sT - ipX} + a_2^*\,e^{s^*T + ipX} \tag{8a}$$

$$b = b_1\,e^{sT - ipX} + \text{c.c.} \tag{8b}$$

The eigenvalues of the linearized operator (7) are the eigenvalues of the 3×3 matrix (m_{ij}) given in the appendix, *i.e.* are solutions of the dispersion relation:

$$s^3 + f\,(p)\,s^2 + g\,(p)\,s + h\,(p) = 0. \tag{9}$$

The functions $f\,(p)$, $g\,(p)$ and $h\,(p)$ are polynomials in p, whose coefficients depend on the parameters q, c_1, c_2, κ_r, κ_i, $(\varepsilon^{-1}\delta)$, $(\varepsilon^{-1}c)$ and χ. At this stage, no assumption has been made about the magnitude of the perturbation wavenumber p. Thus, the roots of the dispersion relation can be obtained using Cardan formulas for any p. Nevertheless, taking into account the great number of the parameters, the discussion of the sign of the real part of these roots is intractable. Moreover, experimental observations show that secondary instabilities arise from the long wave instability, *i.e.* $p \ll 1$.

For long wavelength disturbances ($p \ll 1$), the eigenvalues can be expanded in powers of p, and solved for the successive orders. One obtains:

$$s_1 = -2\,(1 - q^2) + i\,[\alpha\,(\varepsilon^{-1}\,c) + 2\,(c_1 + c_2)\,q]\,p + O\,(p^2) \tag{10}$$

$$s_{2,3} = \frac{i}{2}\,[2\,(c_1 - c_2)\,q - (1 + \alpha)\,(\varepsilon^{-1}\,c)]\,p \pm \frac{1}{2}\,\Phi\,(q)^{1/2}\,p + \frac{1}{1 - q^2}\,(\Phi_2\,(q) \pm i\,\Phi\,(q)^{-1/2}\,\Phi_3\,(q))\,p^2 + O\,(p^3) \tag{10b}$$

where:

$$\alpha = \frac{\kappa_r\,\delta}{c} = O\,(1), \qquad \beta = \frac{\kappa_i\,\delta}{c} = O\,(1),$$

$$\Phi\,(q) = -4\,(c_1 - c_2)^2\,q^2 + 4\,(\varepsilon^{-1}\,c)\,[2\,\beta - (1 + \alpha)\,c_1 + (1 - \alpha)\,c_2]\,q - (1 + \alpha)^2\,(\varepsilon^{-1}\,c)^2,$$

and where $\Phi_2\,(q)$ and $\Phi_3\,(q)$ are quadratic and cubic polynomials, defined in the appendix.

4. Discussion of the instability criterion

We first recall some results about the stability of the travelling wave solutions (6a) of the classical CGL equation (Benjamin and Feir, 1967; Benney and Newell, 1967; Janiaud, Pumir, Bensimon, Croquette, Richter and Kramer, 1992; Lange and Newell, 1974; Stuart and Di Prima, 1978). This case corresponds to zero coupling coefficients, *i.e.* to $\alpha = \beta = 0$. The linear stability analysis gives two eigenvalues, which can be related to an amplitude mode and a phase mode, the latter corresponding to the translational invariance of the CGL equation. The amplitude mode is always stable. Thus, the stability of the travelling wave only depends on the phase mode, which can be unstable, depending on the parameters q, c_1, c_2. The results are the following (*Fig.* 4):

a) The travelling wave with wavenumber $k = k_c\,(q = 0)$ is unstable if:

$$1 + c_1\,c_2 < 0 \quad \text{(Benjamin-Feir instability)}. \tag{11}$$

This criterion for the "generalized Benjamin-Feir instability" has been obtained by Lange & Newell.

b) A travelling wave with wavenumber $k \neq k_c\,(q \neq 0)$

- is always unstable in the Benjamin-Feir unstable domain $(1 + c_1\,c_2 < 0)$;
- is unstable in the Benjamin-Feir stable domain $(1 + c_1\,c_2 > 0)$ if:

$$q_c^2 < q^2 < 1 \quad \text{(Eckhaus instability)}, \tag{12}$$

i.e.

$$q_c^2\,\nu\,(R - R_c)/R_c/\xi^2 < (k - k_c)^2 < \nu\,(R - R_c)/R_c/\xi^2,$$

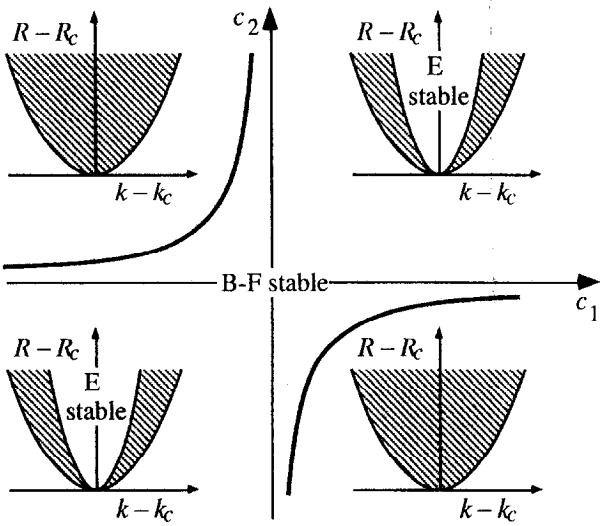

Fig. 4. – The Benjamin-Feir (B-F) stable and unstable domains lie inside and outside the Lange & Newell hyperbola. In the B-F unstable domain, all travelling waves are unstable (hatched region). In the B-F stable domain, the stable travelling waves lie inside the Eckhaus parabola.

where

$$q_c^2 = \frac{1 + c_1 c_2}{3 + c_1 c_2 + 2 c_2^2}.$$

These instabilities come from the existence of a neutral phase mode related to the translational invariance of the problem (Pomeau and Manneville, 1979)

For systems involving galilean invariance, Coulet and Fauve (1985) have shown that the dynamics of the neutral phase mode, related to translational invariance, is modified by the coupling with a neutral mean flow mode, related to galilean invariance, and they derived the corresponding phase equations. However, their study applies for systems with space-reflection symmetry only, which corresponds to $c = c_1 = c_2 = \kappa_r = 0$ in (5).

We note that on considering the case $c = O(1)$ and $\delta = O(1)$ in (5), the dominant terms in the amplitude equation (5b) would lead to:

$$B = -\frac{\delta}{c}|A|^2 + Q, \quad \text{with } Q = 1 - q^2.$$

where the integration constant Q has been chosen in order to recover the family of travelling solutions (6a). This equation corresponds to a slaving of the amplitude B to the modulus of A. Inserting this expression for B into (5a), the latter would reduce to the classical CGL equation. Instability criteria would then reduce to the criteria above, (11) and (12), with modified coefficients c_1 and c_2. Thus, even if slaved, the long wave B might stabilize (resp. destabilize) an unstable (resp. stable) travelling wave. Nevertheless, and as already mentioned, the case $c = O(1)$ and $\delta = O(1)$ do not agree with experiments, so we return to the more interesting case $c = O(\varepsilon)$ and $\delta = O(\varepsilon)$.

When the long wave mode B is taken into account with its own dynamics, three eigenvalues (10) arise. The eigenvalue s_1 corresponds to the amplitude mode of the CGL equation. It is always stable, even in the presence of the marginal long-wave mode, and whatever the value of q. Thus, a travelling wave is unstable against long-wavelength disturbances if the real part of s_2 or s_3 is positive. In order to clarify the discussion for the eigenvalues s_2 and s_3, we distinguish two cases: the case $q = 0$, corresponding to the travelling wave with wavenumber $k = k_c$ and the case $q \neq 0$, corresponding to travelling waves with wavenumber $k = k_c + \varepsilon q \nu^{1/2}/\xi$.

4.1. The case $k = k_c\,(q = 0)$

For $q = 0$, the real parts $\sigma_{2,3}$ of the eigenvalues (10b) become:

$$\sigma_2 = \Theta p^2 + O(p^3) \tag{13a}$$

$$\sigma_3 = \Sigma p^2 + O(p^3) \tag{13b}$$

where:

$$\Theta = -(1 + c_1 c_2) + \frac{\alpha c_2 - \beta}{1 + \alpha} c_1$$

$$\Sigma = -\chi + \frac{\alpha (\varepsilon^{-1} c)^2 (1 + \alpha)^2 + 2 c_1 (\beta - 2 \alpha c_2)}{2 (1 + \alpha)}.$$

The eigenvalue s_2 corresponds to the phase mode of the CGL equation. Indeed, in the absence of the neutral mode at $k = 0$ (*i.e.* for $\alpha = \beta = 0$) one recovers the Lange & Newell criterion (11). In the presence of the marginal mode $k = 0$, the instability criterion for the phase mode becomes:

$$\Theta > 0. \tag{14}$$

In the (c_1, c_2)-plane, the corresponding "Benjamin-Feir unstable" domain lies outside an hyperbola, and the "Benjamin-Feir stable" domain lies inside (*Fig.* 5). The coupling between the amplitudes A and B leads to a translation $-\beta$ of the horizontal asymptote and an expansion $(1 + \alpha)$ of the Lange & Newell hyperbola (11). If $1 + \alpha < 0$, the branches of the hyperbola lie in the opposite quadrants.

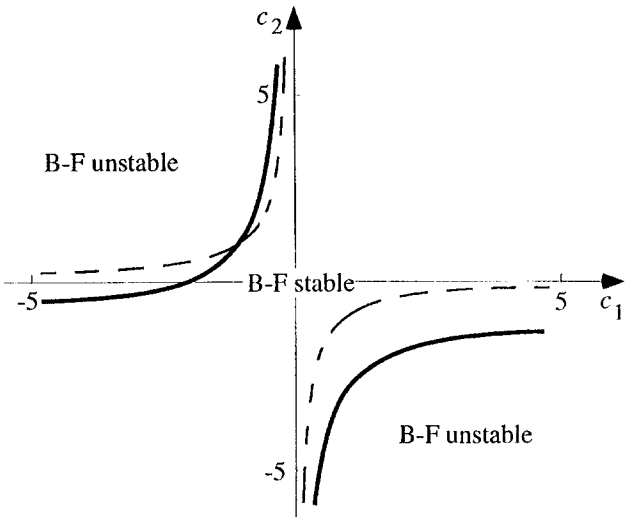

Fig. 5. – Influence of the neutral mode $k = 0$ on the Benjamin-Feir instability domain. (– – –): Lange & Newell's hyperbola; (——): hyperbola $\Theta = 0$ for $\alpha = 1, \beta = 1$.

The eigenvalue s_3 is linked to the neutral mode $k = 0$, since it reduces to $-\chi$ when the coupling coefficients α and β are zero. When the short wave is present, this mode is unstable if:

$$\Sigma > 0. \tag{15}$$

In the (c_1, c_2)-plane, the instability domain lies again outside an hyperbola. This hyperbola is obtained from the Lange & Newell one by a translation $\beta/2\alpha$ of the horizontal asymptote and an expansion $(1 + \alpha)(-2\chi + \alpha(\varepsilon^{-1} c)^2 (1 + \alpha))/4\alpha$.

Finally, the main results of this section are the following:

(i) The mode related to the phase of the complex amplitude A (eigenvalue s_2) may be stabilized (in the Benjamin-Feir unstable domain (11)) or destabilized (in the Benjamin-Feir stable domain) by the coupling with B. In the (c_1, c_2)-plane, the stable domain

lies between the two branches of an hyperbola. The growth rate of this instability is $O(p^2)$ for small p.

(ii) The long wave mode (eigenvalue s_3) may be destabilized by the coupling between A and B. In the (c_1, c_2)-plane, the stable domain lies between the two branches of a second hyperbola. The growth rate of this instability is also $O(p^2)$ for small p for small wavenumber disturbances p.

(iii) The actual stable domain for the travelling wave $k = k_c$ lie within the intersection of the two stable domains defined above.

4.2. The case $k \neq k_c$ $(q \neq 0)$

We now turn to the general case, *i.e.* a travelling wave with wavenumber close to k_c $(q \neq 0)$. The eigenvalues s_2 and s_3 (10b) shows that instability can occur either at order p or at order p^2, depending on the sign of $\Phi(q)$.

On the one hand, when $\Phi(q) > 0$, the real parts $\sigma_{2,3}$ of the eigenvalues (10b) become:

$$\sigma_{2,3} = \pm\frac{1}{2}\sqrt{\Phi(q)}\,p + O(p^2). \tag{16}$$

One of the eigenvalues has a positive real part, and the travelling wave with wavenumber $k(q)$, $|q| < 1$, is unstable against long wavelength disturbances. The order of magnitude of the growth rate is $O(p)$.

On the other hand, when $\Phi(q) < 0$, the $O(p)$ term involving $\Phi(q)$ in (10b) is imaginary, and the real parts $\sigma_{2,3}$ of the eigenvalues now become:

$$\sigma_{2,3} = \frac{\Psi(q)}{1-q^2}\,p^2 + O(p^3) \tag{17}$$

with

$$\Psi(q) = \Phi_2(q) \pm \frac{\Phi_3(q)}{\sqrt{-\Phi(q)}}.$$

The order of magnitude of the growth rate is p^2.

Instability at order p $(\Phi(q) > 0)$

We first consider the possibility of instability at order p, for which the real part of the eigenvalues is given by (16). Inspection of the quadratic polynomial $\Phi(q)$ show that $\Phi(q) > 0$ requires its discriminant Δ to be positive. This discriminant is given by:

$$\Delta = 64\,(\varepsilon^{-1}c)^2\,(c_2 + \beta - c_1(1+\alpha))\,(\beta - \alpha c_2). \tag{18}$$

Indeed, if Δ is negative, $\Phi(q)$ has no real root, and is always negative. If Δ is positive, $\Phi(q)$ has two real roots q_1 and q_2 with same sign, in between it is positive. The corresponding domains in the (c_1, c_2)-plane are sketched on Figure 6, for given α and β. As an example, the variation of the bandwidth $[q_1, q_2]$ versus c_1 is shown in Figure 7.

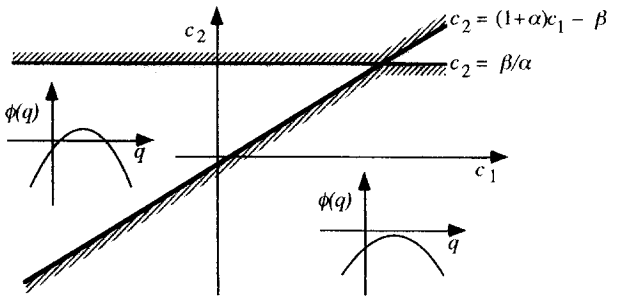

Fig. 6. – Inside the hatched region: no long-wave instability at order p; outside the hatched region: the band $[q_1, q_2]$ is unstable. This figure corresponds to $\alpha > 0$, $\beta > 0$.

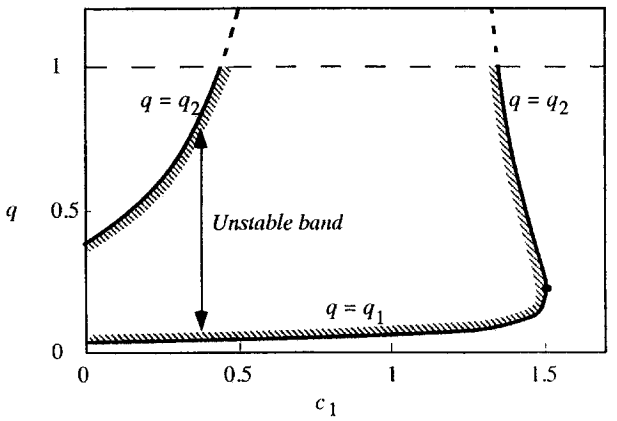

Fig. 7. – Unstable band at $O(p)$ versus c_1 for $\alpha = 1$, $\beta = 2$, $c = 0.1$, $c_2 = 1$. Beyond $c_1 = 1.5$, $\phi(q)$ has no root in $[-1, 1]$ and all travelling waves are stable.

For the chosen values of the other parameters, it can be seen that for $c_1 < 1.5$, Δ is positive and travelling waves such that $q_1 < q < q_2 < 1$ are unstable. For $c_1 > 1.5$, Δ is negative and all travelling waves are stable at order p.

Thus, there exist unstable travelling waves at order p if and only if:

$$\Delta > 0, \quad [q_1, q_2] \cap [-1, 0] \neq \varnothing \quad \text{or} \quad [q_1, q_2] \cap [0, 1] \neq \varnothing. \tag{19}$$

When conditions (19) hold, two different cases may be distinguished, depending on the values of q_1 and q_2. For positive roots, these two cases are as follows:

(a) $0 \leq q_1 < q_2 < 1$: the unstable travelling waves are such that (*Fig.* 8*a*):

$$q_1 (\nu (R - R_c)/R_c)^{1/2}/\xi < k - k_c < q_2 (\nu (R - R_c)/R_c)^{1/2}/\xi.$$

(b) $0 \leq q_1 < 1 < q_2$: the unstable travelling waves are such that (*Fig.* 8*b*):

$$q_1 (\nu (R - R_c)/R_c)^{1/2}/\xi < k - k_c < (\nu (R - R_c)/R_c)^{1/2}/\xi,$$

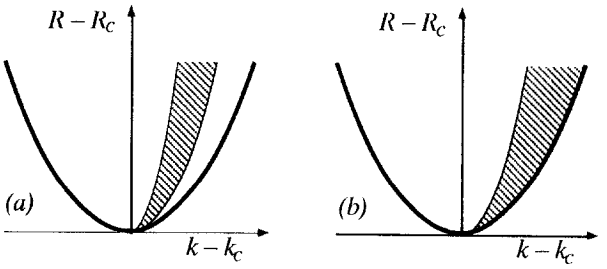

Fig. 8. – Bold parabola: linear stability boundary, from the dispersion relation (3); hatched regions: unstable waves at $O(p)$. (*a*): $0 \leq q_1 < q_2 < 1$; (*b*) $0 \leq q_1 < 1 < q_2$.

Note that $q_1 = 0$ is obtained for $\alpha = -1$ only. For negative roots, similar conclusions hold, with an unstable band for $k < k_c$. Thus, the topology of the bands of unstable wavenumbers is qualitatively different from those of the classical Eckhaus instability. First, the unstable band exists for $k < k_c$ *or* for $k > k_c$: the symmetry of the classical Eckhaus parabola is broken. Second, a stable band may lie between the marginal stability parabola and the unstable band. Last but not least, the growth rate of instability is of order p, whereas it is only of order p^2 for the classical Eckhaus instability. Finally, it is important to note that outside the unstable band (*i.e.* for $\Phi(q) < 0$), travelling waves are not necessarily stable. Indeed, in this case, their stability depends on the sign of the term of order p^2.

Instability at order p^2 $(\Phi(q) < 0)$

We now consider the case $\Phi(q) < 0$ for $|q| < 1$. The real parts of the eigenvalues are given by (17) and the travelling wave with wavenumber $k(q)$ is unstable when $\Psi(q) > 0$. Here, no simple instability criterion such as (19) can be given, because the analysis turns out to be too complicated. Nevertheless, the following features can be delineated. The equation $\Psi(q) = 0$ may have 0, 2, 4 or 6 real roots. When $\Psi(q) \to -\infty$ for $p \to \pm\infty$, these roots define 0, 1, 2 and 3 bands of unstable wavenumbers, respectively; when $\Psi(q) \to +\infty$ for $p \to \pm\infty$, these roots define 1, 2, 3 and 4 bands of unstable wavenumbers, respectively (some of these bands may correspond to $|q| > 1$ and should not be taken into account). These bands are not symmetric about the $q = 0$ axis. Furthermore, one of them may contain the $q = 0$ axis. These bands define parabolas in the $(k - k_c, R - R_c)$ plane, in between travelling waves are unstable.

The stable and unstable bands of wavenumber at order p^2 are shown on Figure 9, for the two extreme cases: no roots and six roots in the range $[-1, 1]$. If $\Psi(q)$ has *no real root* in the range $[-1, 1]$, all travelling waves stable if $\Psi(q) < 0$ (*Fig.* 9*a*), or unstable if $\Psi(q) > 0$ (*Fig.* 9*b*). If $\Psi(q)$ has *six real roots* in the range $[-1, 1]$, there are four unstable bands if $\Psi(q) \to +\infty$ for $p \to \pm\infty$ (*Fig.* 9*c*), or three unstable bands if $\Psi(q) \to -\infty$ for $p \to \pm\infty$ (*Fig.* 9*d*).

Finally, the complete stability diagram for travelling waves against long wavelength perturbations is obtained by combining the stability diagrams at order p and at order p^2. If the instability criterion (19) at order p is satisfied, there exist unstable travelling waves with growth rate $O(p)$. If the instability criterion at order p is *not* satisfied, the

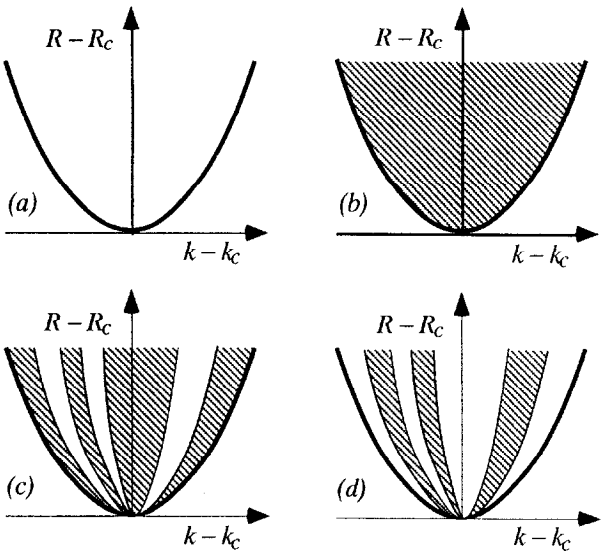

Fig. 9. – Bold parabola: linear stability boundary; hatched regions: unstable travelling waves at order p^2. (*a*): $\psi(q) < 0$ has no real root in $[-1, 1]$; (*b*): $\psi(q) > 0$ has no real root in $[-1, 1]$; (*c*): $\psi(q)$ has six real roots in $[-1, 1]$, and $\psi(q) \to +\infty$ for $p \to \pm\infty$; (*d*): $\psi(q)$ has six real roots in $[-1, 1]$, and $\psi(q) \to -\infty$ for $p \to \pm\infty$.

instability criterion at order p^2 must be considered, and if it is satisfied, the instability growth rate is $O(p^2)$.

5. Summary and discussion

In the present work, we have studied the stability of interfacial travelling waves against long wavelength disturbances. The weakly nonlinear dynamics is governed by a set of two coupled amplitude equations: one for the envelope A of the travelling wave with finite wavenumber, and the other for the amplitude B of the neutral mode $k = 0$. We considered the case corresponding to nearly equal group velocity of the wave packet A and wave velocity of the mode B, which corresponds to experimental observations. The conclusions are then the following.

Three eigenvalues arise from the linear stability analysis of travelling waves. Two of them correspond to the stable amplitude mode and the phase mode of the complex Ginzburg-Landau (CGL) equation. The third one corresponds to the long wave mode.

For the travelling wave with wavenumber $k = k_c$, the Benjamin-Feir instability is recovered. In the (c_1, c_2)-plane, the marginal phase mode and long wave mode each define an hyperbola similar to the Lange & Newell hyperbola, separating the Benjamin-Feir stable and unstable domains. The actual stable domain for the travelling wave $k = k_c$ lies within the intersection of the two stable domains bounded by the two hyperbolas.

For travelling waves with wavenumber $k \neq k_c$, which is the general case, new important features arise and are the main results of this paper. For long wavelength perturbations with wavenumber p, instability can arise either at order p or at order p^2. The resulting stability diagram is characterized by the possible existence of several

parabolic non-symmetric bands of unstable wavenumbers, separated by stable bands. Unlike the case of the classical Eckhaus instability, which occurs at order p^2 only, these unstable bands do not necessarily lean on the marginal stability parabola, and then can lie entirely inside this parabola. This essential feature enables the observation of long wavelength instability either increasing or decreasing the control parameter R. Recent experimental observations by Barthelet and Charru (1996) may be explained within the frame of these theoretical results.

The physical mechanism of the instability can be described as follows. The key is that any finite-amplitude wave drags fluid (Stokes drift), with induced-flow rate proportional to $k|A|^2$ (Batchelor, 1967). Consider a travelling wave which would be Eckhaus-stable in the absence of the long wave mode. Any small gradient of the induced-flow rate induces a local variation of the mean interface position B, due to mass conservation (δ-term in (5b)). This variation of the mean interface position modifies the local wavenumber and the modulus $|A|$ of the amplitude through the κ-term in (5a), and the induced-flow rate. Finally, if this feedback mechanism is positive, the initial perturbation of the induced-flow rate is amplified and the travelling wave is unstable. Of course, the final state resulting from this instability cannot be described by linear analysis. Nevertheless, experiments indicate that it eventually leads to wavelength annihilation, as shown in Figure 3.

The above mechanism is very close to that described by Chang *et al.* (1997), who analyse wavenumber selection for periodic solutions of the Kuramoto-Sivashinsky equation with an additional linear dispersive term. Moreover, their numerical simulations strongly resemble the experimental results shown on Figure 2. However, we believe that equations (5) are more relevant to the problem of interfacial waves in viscous two-layer shear flows than the "generalized" KS equation. Indeed, the KS equation describes wave dynamics in the small wavenumber limit only, and leads to the dispersion relation (1) showing a large band of unstable waveumbers including zero, as displayed on Figure 2*a*. On the other hand, our experimental observations show short waves with wavelength close to the fluid layer thickness. Moreover, the wavenumber selected by the secondary instability is close to the initial one, contrary to the Chang *et al.* simulations.

Finally, the amplitude equations (5) arising in the physical context of interfacial waves in two-layer flows can be considered as normal forms for other problems with translational and galilean invariances, with no space-reflection symmetry. These two invariances lead to marginal phase mode and long wave mode, whose coupling leads to very rich dynamics.

APPENDIX

Matrix (m_{ij}) of the linearized operator (7) and the polynomials of (10)

$$m_{11} = -(1+ic_1)(q-p)^2 + (1+ic_2)(2q^2-1) + i(c_1-c_2)q^2$$

$$m_{12} = m_{21}^* = -(1+ic_2)(1-q^2)$$

$$m_{13} = m_{23}^{*} = \kappa_r + i\,\kappa_i$$

$$m_{22} = -(1 - ic_1)\,(q + p)^2 + (1 - ic_2)\,(2\,q^2 - 1) - i\,(c_1 - c_2)\,q^2$$

$$m_{31} = m_{32} = -i\,(\varepsilon^{-1}\,\delta)\,(1 - q^2)\,p$$

$$m_{33} = -i\,(\varepsilon^{-1}\,c)\,p - \chi\,p^2,$$

$$2\,\Phi_2\,(q) = q^2\,(3 + c_1\,c_2 + 2\,c_2^2 + \chi) + q\,(\varepsilon^{-1}\,c)\,(-\beta + \alpha\,c_1 + 2\,\alpha\,c_2) - \left(1 + c_1\,c_2 - \frac{1}{2}\,\alpha\,(1 + \alpha)\,(\varepsilon^{-1}\,c)^2 + \chi\right)$$

$$\begin{aligned} 2\,\Phi_3\,(q) = {} & 2\,q^3\,(c_2 - c_1)\,(3 + c_1\,c_2 + 2\,c_2^2 - \chi) \\ & + q^2\,(\varepsilon^{-1}\,c)(\alpha - 3 - 4\,\beta\,c_1 - 6\,\beta\,c_2 + 2\,\alpha\,c_1^2 + c_2^2\,(6\,\alpha - 2) \\ & + c_1\,c_2\,(3\,\alpha - 1) + (1 + \alpha)\,\chi) \\ & + q\,((\varepsilon^{-1}\,c)^2\,(-\beta - 3\,\alpha\,\beta + 2\,\alpha\,(1 + \alpha)\,c_1 + \alpha\,(1 + 3\,\alpha)\,c_2) \\ & + 2\,(c_1 - c_2)\,(1 + c_1\,c_2 - \chi)) \\ & + (\varepsilon^{-1}\,c)\left(\frac{1}{2}\,(\varepsilon^{-1}\,c)^2\,\alpha\,(1 + \alpha)^2 + 1 + \alpha + 2\,\beta\,c_1 + (1 - \alpha)\,c_1\,c_2 - (1 + \alpha)\,\chi\right) \end{aligned}$$

REFERENCES

ALBERT F., 1996, *Stabilité d'une interface entre deux fluides cisaillés : étude numérique et asymptotique*, Thèse de Doctorat, Institut National Polytechnique de Toulouse, France.

BARTHELET P., CHARRU F., 1996, Secondary instabilities of interfacial waves in a two-layer Couette flow, EUROMECH Colloquium 355, *Interfacial Instabilities*, Palaiseau, France.

BARTHELET P., CHARRU F., FABRE J., 1995, Experimental study of interfacial long waves in a two-layer shear flow, *J. Fluid Mech.*, **303**, 23-53.

BATCHELOR G. K., 1967, *An introduction to fluid dynamics*, Cambridge University Press.

BENJAMIN T. B., FEIR J. E., 1967, The disintegration of wave trains on deep water, *J. Fluid Mech.*, **27**, 417-430.

BENNEY D. J., NEWELL A. C., 1967, The propagation of non-linear wave envelopes, *J. Math. Phys.*, **46**, 133-145.

CHANG H.-C., DEMEKHIN E. A., KOPELEVICH D. I., YE Y., 1997, Nonlinear Wavenumber Selection in Gradient Flow Systems, *Phys. Rev. E*, **55**, 2818-2834.

CHARRU F., FABRE J., 1994, Long waves at the interface between two viscous fluids, *Phys. Fluids*, **6**, 1223-1235.

COULLET P., FAUVE S., 1985, Propagative phase dynamics for systems with galilean invariance, *Phys. Rev. Lett.*, **55**, 2857-2859.

HOOPER A. P., 1985, Long-wave instability at the interface between two viscous fluids: Thin layer effects, *Phys. Fluids*, **28**, 1613-1618.

HOOPER A. P., GRIMSHAW R., 1985, Nonlinear instability at the interface between two viscous fluids, *Phys. Fluids*, **28**, 37-45.

JANIAUD B., PUMIR A., BENSIMON D., CROQUETTE V., RICHTER H., KRAMER L., 1992, The Eckhaus instability for travelling waves, *Physica D*, **55**, 269-286.

LANGE C. G., NEWELL A. C., 1974, A stability criterion for envelope equations, *SIAM J. Appl. Math.*, **27**, 441-456.

NEWELL A. C., PASSOT T., LEGA J., 1993, Order parameter equations for patterns, *Annu. Rev. Fluid Mech.*, **25**, 399-453.

POCHEAU A., DAVIAUD F., 1997, Sensitivity of convective structures to mean flow boundary conditions: A correlation between symmetry and dynamics, *Phys. Rev. E*, **55**, 353-373.

POMEAU Y., MANNEVILLE P., 1979, Stability and fluctuations of a spatially periodic convective flow, *J. Phys. (Paris)*, **40**, 609-612.

RENARDY M., RENARDY Y., 1993, Derivation of amplitude equations and analysis of sideband instabilities in two-layer flows, *Phys. Fluids A*, **5**, 2738-2762.

RENARDY Y., 1985, Instability at the interface between two shearing fluid in a channel, *Phys. Fluids*, **28**, 3441-3443.

RIECKE H., 1992, Self-trapping of traveling wave pulses in binary mixture convection, *Phys. Rev. Lett.*, **68**, 301-304.

STUART J. T., DI PRIMA R. C., 1978, The Eckhaus and Benjamin-Feir resonance mechanisms, *Proc. Roy. Soc. London A*, **362**, 27-41.

WHITHAM G. B., 1974, *Linear and Nonlinear Waves*, Wiley, New York.

YIH C. S., 1967, Instability due to viscous stratification, *J. Fluid Mech.*, **27**, 337-352.

ZIPPELIUS A., SIGGIA E. D., 1983, Stability of finite-amplitude convection, *Phys. Fluids*, **26**, 2905-2915.

(Manuscript received and accepted May 1997.)